

Orbital Order in Two-Orbital Hubbard Model

Kojiro Honkawa¹ and Seiichiro Onari^{1,2*}

¹*Department of Physics, Okayama University, Okayama 700-8530, Japan*

²*Research Institute for Interdisciplinary Science, Okayama University, Okayama 700-8530, Japan*

In strongly correlated multiorbital systems, various ordered phases appear. In particular, the orbital order in iron-based superconductors attracts much attention since it is considered to be the origin of the nematic state. To clarify the essential conditions for realizing orbital orders, we study the simple two-orbital (d_{xz} , d_{yz}) Hubbard model. We find that the orbital order, which corresponds to the nematic order, appears due to the vertex corrections even in the two-orbital model. Thus, the d_{xy} orbital is not essential to realize the nematic orbital order. The obtained orbital order is determined by the orbital dependence and the topology of Fermi surfaces. We also find that another type of orbital order, which is rotated 45° , appears in a heavily hole-doped case.

1. Introduction

In the phase diagram of iron-based superconductors, the electronic nematic state with C_2 symmetry appears universally under the structural phase transition temperature T_S , and the superconducting state emerges next to the nematic state.^{1,2)} The origin of the nematic state has stimulated much attention since the mechanism of superconductivity would be strongly related to the mechanism of the nematic state. To explain the nematic order and fluctuations, both the spin-nematic scenario^{3,4)} and the orbital-order scenario^{5–11)} have been proposed. In the former scenario, the origin of the nematic state is the spin-nematic order. The spin-fluctuation-induced spin-nematic order appears slightly above the magnetic transition temperature when the magnetic frustration is strong. However, the nematic state in FeSe with small spin fluctuations cannot be explained by the spin-nematic scenario. In the latter scenario, the origin is the ferro-orbital order ($n_{xz} \neq n_{yz}$), which is caused by the vertex correction (VC) of the Coulomb interaction.^{5,6)} By applying the self-consistent VC (SC-VC) method to

*onari@okayama-u.ac.jp

the realistic five Fe d orbital model based on first-principles calculation, the nematic state in both LaFeAsO and FeSe has been naturally reproduced.^{6,12)}

Recently, the remarkable \mathbf{k} dependence of the orbital polarization, which cannot be explained using the mean-field theory, has been observed in FeSe.¹³⁾ The \mathbf{k} dependence of the orbital polarization is also reproduced in the orbital-order scenario.¹⁴⁾ In addition, the s -wave state without sign reversal (s_{++} -wave state) mediated by the orbital fluctuations has also been proposed in iron-based superconductors.^{5-8,15,16)} The SC-VC theory had also succeeded in explaining other multiorbital systems such as the nematic CDW in cuprates,^{17,18)} the nematic state in Sr₃Ru₂O₇,¹⁹⁾ and the spin-triplet superconductivity in Sr₂RuO₄.^{20,21)}

In our previous work based on the SC-VC theory in realistic five-orbital models of iron-based superconductors, we have found that the nematic orbital order $n_{xz} \neq n_{yz}$ is caused by the VC including d_{xz} , d_{yz} , and d_{xy} orbitals.^{6,12)} In the five-orbital models, Fermi surfaces (FSs) are composed of d_{xz} , d_{yz} and d_{xy} orbitals. Thus, these orbitals are expected to be important in realizing the nematic orbital order. However, the necessary conditions for the orbital order are yet unclear. In order to clarify the essence of the orbital order, we study the simple two-orbital (d_{xz} , d_{yz}) model systematically by the SC-VC method.

We found that the VC for the orbital susceptibility is also enhanced in the simple two-orbital model, and that the nematic orbital order appears similarly to the case of the realistic five-orbital models. Thus, the d_{xy} orbital is not essential to realize the nematic orbital order. We also found that another type of orbital order, which corresponds to the 45°-rotated orbital order, appears when the holes are heavily doped. The obtained orbital order is determined by the orbital dependence and the topology of the FSs.

2. Formulation

We study a simple two-orbital (d_{xz} , d_{yz}) Hubbard model in a square lattice. The Hamiltonian is given as

$$H = \sum_{\mathbf{k}} \sum_{l,m=1,2} \sum_{\sigma=\uparrow,\downarrow} \xi_{\mathbf{k}}^{lm} c_{\mathbf{k},l,\sigma}^{\dagger} c_{\mathbf{k},m,\sigma} + H_{\text{int}}, \quad (1)$$

where $l, m = 1, 2$ represents the orbital; $1 = d_{xz}$ and $2 = d_{yz}$. In the tight-binding model, we employ the dispersion relation²²⁾ $\xi_{\mathbf{k}}^{11} = -2t_1 \cos(k_x) - 2t_2 \cos(k_y) - 4t_3 \cos(k_x) \cos(k_y)$, $\xi_{\mathbf{k}}^{22} = -2t_2 \cos(k_x) - 2t_1 \cos(k_y) - 4t_3 \cos(k_x) \cos(k_y)$, and $\xi_{\mathbf{k}}^{12} = \xi_{\mathbf{k}}^{21} = -4t_4 \sin(k_x) \sin(k_y)$. We control the band filling n systematically, where $n = 1$ corresponds to the half-filling. H_{int} is the multiorbital Coulomb interaction including the intra (inter) orbital interaction U (U') and the exchange interaction J . Hereafter, we use the relation $U = U' + 2J$ from rotational

invariance. The irreducible susceptibility in the orbital representation without the VC is given as $\chi_{ll',mm'}^0(q) = -\frac{T}{N} \sum_k G_{lm}(k+q)G_{m'l'}(k)$, where G is the Green's function, and q and k are denoted as $q = (\mathbf{q}, \omega_n = 2n\pi T)$ and $k = (\mathbf{k}, \epsilon_n = (2n+1)\pi T)$, respectively. We take $N = 64 \times 64$ \mathbf{k} meshes and 256 Matsubara frequencies. Using the RPA, the matrix of the spin (orbital) susceptibility is given as

$$\hat{\chi}^{s(c)}(q) = \hat{\chi}^0(q) \left[1 - \hat{\Gamma}^{s(c)} \hat{\chi}^0(q) \right]^{-1}, \quad (2)$$

where $\hat{\Gamma}^{s(c)}$ denotes the bare Coulomb interaction for spin (charge) channel given by

$$\Gamma_{l_1 l_2, l_3 l_4}^{s(c)} = \begin{cases} U(-U), & l_1 = l_2 = l_3 = l_4 \\ U'(U' - 2J), & l_1 = l_3 \neq l_2 = l_4 \\ J(-2U' + J), & l_1 = l_2 \neq l_3 = l_4 \\ J(-J), & l_1 = l_4 \neq l_2 = l_3 \end{cases}. \quad (3)$$

By introducing the VC \hat{X}^c for the orbital channel, the matrix of the orbital susceptibility is given by

$$\hat{\chi}^c(q) = \left[\hat{\chi}^0(q) + \hat{X}^c(q) \right] \left[1 - \hat{\Gamma}^c \left\{ \hat{\chi}^0(q) + \hat{X}^c(q) \right\} \right]^{-1}. \quad (4)$$

In this study, we neglect the VC \hat{X}^s for the spin channel for simplicity since \hat{X}^s is smaller than \hat{X}^c , as reported previously.⁵⁾ The spin Stoner factor α_s is given by the maximum eigenvalue of $\hat{\Gamma}^s \hat{\chi}^0(\mathbf{q}, 0)$, while the charge Stoner factor α_c is given by the maximum eigenvalue of $\hat{\Gamma}^c \left[\hat{\chi}^0(\mathbf{q}, 0) + \hat{X}^c(\mathbf{q}, 0) \right]$. The ordered state is realized when $\alpha_s = 1$ or $\alpha_c = 1$.

The RPA is recovered by putting $\hat{X}^c = 0$. It is clear that $\hat{\chi}^c(q)$ is enhanced over the value in the RPA when $\hat{X}^c(q)$ is large. In the SC-VC method, $\hat{\chi}^{c,s}$ and \hat{X}^c are obtained self-consistently. The VC is given by the Maki-Thompson (MT) and Aslamazov-Larkin (AL) terms, which are the first- and second-order terms, respectively, with respect to $\hat{\chi}^{s(c)}$. The MT term for the orbital susceptibility $X_{ll',mm'}^{\text{MT},c}(q)$ is given by

$$X_{ll',mm'}^{\text{MT},c}(q) = -\left(\frac{T}{N}\right)^2 \sum_{k,k'} \sum_{a,b,c,d} G_{la}(k+q)G_{c'l'}(k)G_{bm}(k'+q)G_{m'd}(k') \left[\frac{1}{2}V_{ab,cd}^c(k-k') + \frac{3}{2}V_{ab,cd}^s(k-k') - \frac{1}{2}\Gamma_{ab,cd}^c - \frac{3}{2}\Gamma_{ab,cd}^s \right], \quad (5)$$

where $\hat{V}^{s,c}(q) \equiv \hat{\Gamma}^{s,c} + \hat{\Gamma}^{s,c} \hat{\chi}^{s,c}(q) \hat{\Gamma}^{s,c}$.

The AL term for the orbital susceptibility $X_{ll',mm'}^{\text{AL},c}(q)$ is given by

$$X_{ll',mm'}^{\text{AL},c}(q) = \frac{T}{N} \sum_{q'} \sum_{a \sim h} \Lambda_{ll',ab,ef}(q; q') \left[\frac{3}{2}V_{ab,cd}^s(q+q')V_{ef,gh}^s(-q') \right]$$

$$+\frac{1}{2}V_{ab,cd}^c(q+q')V_{ef,gh}^c(-q')\Big]\Lambda'_{mm',cd,gh}(q;q'), \quad (6)$$

where the three-point vertex $\hat{\Lambda}(q; q')$ is given as

$$\Lambda_{ll',ab,ef}(q;q') = -\frac{T}{N} \sum_k G_{la}(k+q)G_{fl'}(k)G_{be}(k-q'), \quad (7)$$

and $\Lambda'_{mm',cd,gh}(q;q') \equiv \Lambda_{ch,mg,dm'}(q;q') + \Lambda_{gd,mc,hm'}(q;-q-q')$. When we calculate the total VC, we subtract the double-counting U^2 -terms in Eqs. (5) and (6).²³⁾ By calculating the above equations self-consistently, we find that the MT and U^2 -terms are much smaller than the AL terms.

Here, we introduce the diagonal charge quadrupole susceptibilities as

$$\chi_\gamma^Q(q) = \sum_{ll'} \sum_{mm'} O_\gamma^{l,l'} \chi_{ll',mm'}^c(q) O_\gamma^{m,m'}, \quad (8)$$

where $O_\gamma^{l,m} \equiv \langle l|\hat{O}_\gamma|m\rangle$ is the matrix element of the γ -type quadrupole operator. In the present two-orbital system, $O_{x^2-y^2}^{1,1} = -O_{x^2-y^2}^{2,2} = 1$, $O_{xy}^{1,2} = O_{xy}^{2,1} = 1$, and $O_{3z^2-r^2}^{1,1} = O_{3z^2-r^2}^{2,2} = 1/2$, while other matrix elements are zero. The nematic state with $n_{xz} \neq n_{yz}$ is explained by the divergent of $\chi_{x^2-y^2}^Q(\mathbf{q} = \mathbf{0}, 0)$.^{5,6)} In the two-orbital system without the d_{xy} orbital, $\chi_{3z^2-r^2}^Q$ is identical to the charge susceptibility. Thus, the enhancement of $\chi_{3z^2-r^2}^Q$ driven by the d_{xy} orbital in the five-orbital model⁶⁾ is not realized in the two-orbital system.

Hereafter, we fix the temperature $T = 0.05$ and $J/U = 0.05$. Although $J/U = 0.05$ is smaller than the value obtained by the first-principles calculation,²⁴⁾ we note that the obtained orbital fluctuations without the self-energy for a small $J/U \sim 0.05$ are similar to those including the self-energy for a large $J/U \sim 0.14$ in the five-orbital system.⁶⁾ The VC for the orbital fluctuations is underestimated in the system without the self-energy since U is underestimated.

3. Results and Discussion

We employ the two-orbital tight-binding model of iron-based superconductors with $t_1 = -1$, $t_2 = 1.39$, and $t_3 = t_4 = -0.85$, which is similar to the model given in Ref. 22. First, we calculate the susceptibilities near the ordered state by the SC-VC method. Figure 1 shows U as a function of n , where $\alpha_s = 0.97$ or $\alpha_c = 0.97$ is satisfied for each n . In the blue region, $\alpha_s = 0.97$ is satisfied and spin fluctuations are dominant. In the red (green) region, $\alpha_c = 0.97$ is satisfied and $x^2 - y^2$ -type (xy -type) charge quadrupole fluctuations are dominant. In this model, the $3z^2 - r^2$ -type charge quadrupole susceptibility, which is identical to the charge susceptibility, is much smaller than other susceptibilities. In Fig. 1, the small U indicates that the corresponding ordered state is easily realized. Although we cannot access

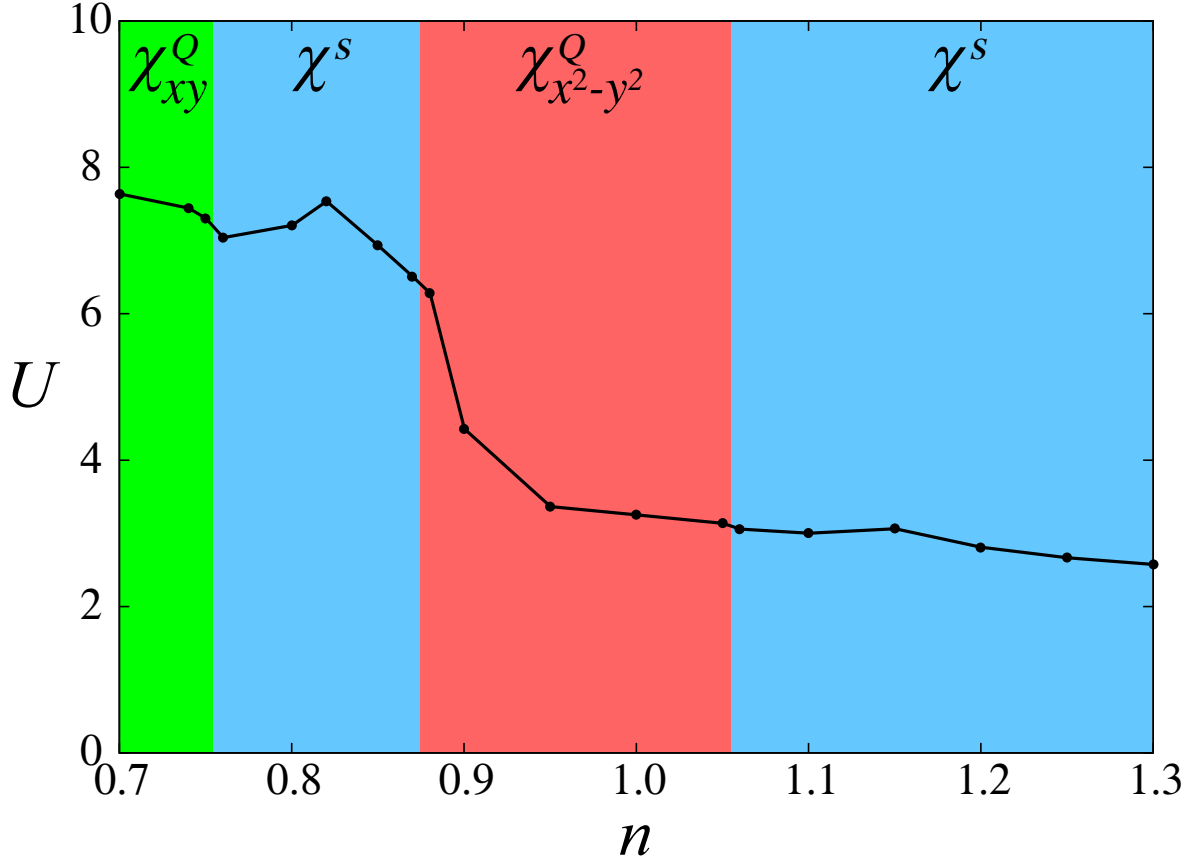


Fig. 1. (Color online) U as a function of band filling n , where $\alpha_{s(c)} = 0.97$ is satisfied for each n . In the blue region, the spin fluctuations are dominant. In the red (green) region, the $x^2 - y^2$ -type (xy -type) charge quadrupole fluctuations are dominant.

$\alpha_{s(c)} > 0.98$ in order to maintain the calculation accuracy, we confirmed that the dominant fluctuations are basically independent of $\alpha_{s(c)}$ for $0.98 \geq \alpha_{s(c)} \geq 0.95$. Only the boundary of the regions slightly depends on $\alpha_{s(c)}$. For $n = 1.0$, the $x^2 - y^2$ -type charge quadrupole fluctuation with the peak at $\mathbf{q} = (0, 0)$ is dominant over the spin fluctuations and the xy -type charge quadrupole fluctuations. This result is consistent with the phase diagram of iron-based superconductors, where the nematic $x^2 - y^2$ -type charge quadrupole (orbital) order appears at higher temperatures than at which the spin order appears.

In Fig. 2(a), we show FSs composed of orbital 1 (green line) and orbital 2 (red line) for $n = 1.0$. The FSs around $\mathbf{k} = (0, 0)$ and $\mathbf{k} = (\pi, \pi)$ are the hole FSs, while the FSs around $\mathbf{k} = (\pi, 0)$ and $\mathbf{k} = (0, \pi)$ are the electron FSs. These FSs are consistent with the FSs of iron-based superconductors except for the FS around $\mathbf{k} = (\pi, \pi)$, which is composed of d_{xy} orbital in iron-based superconductors. Figures 2(b)–2(d) show the \mathbf{q} dependences of $\chi^s(\mathbf{q}, 0)$, $\chi_{x^2-y^2}^Q(\mathbf{q}, 0)$, and $\chi_{xy}^Q(\mathbf{q}, 0)$, respectively. $\chi^s(\mathbf{q}, 0)$ has a peak at $\mathbf{q} = (\pi, 0), (0, \pi)$ due to the

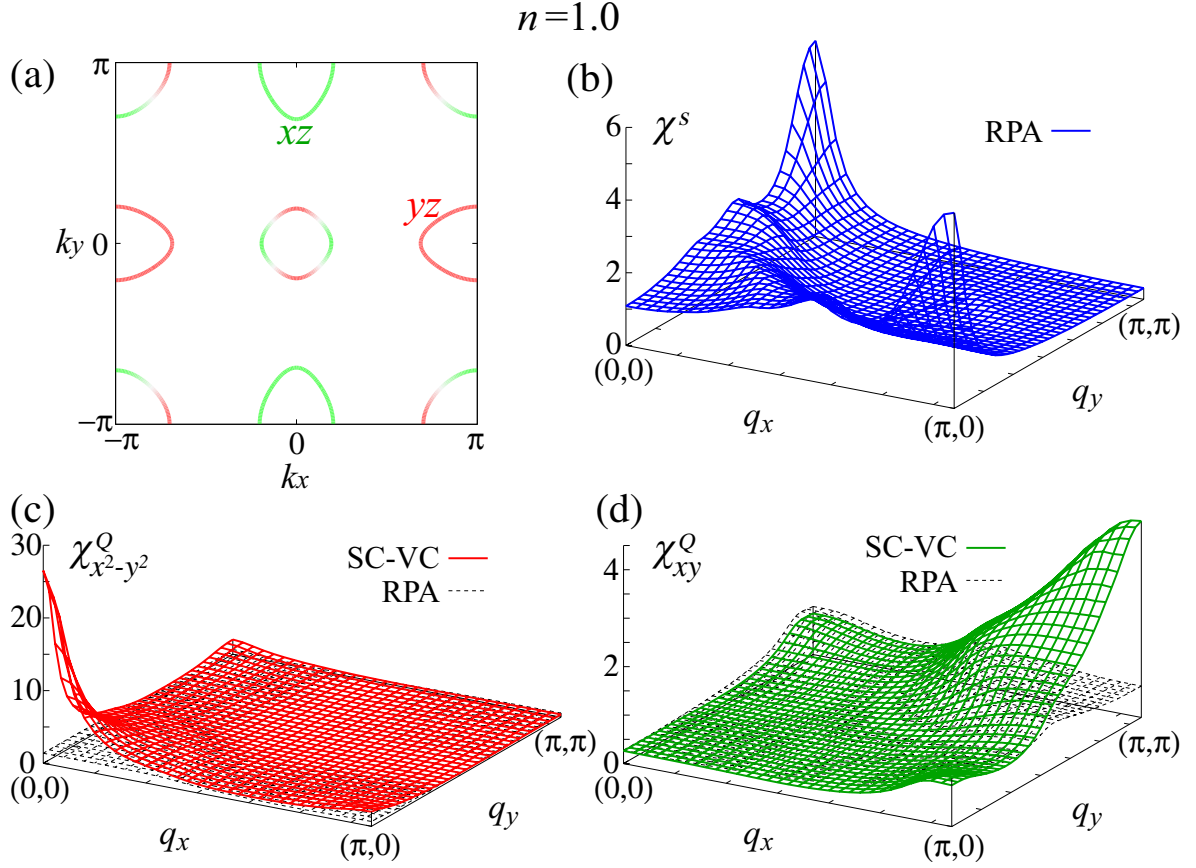


Fig. 2. (Color online) (a) FS composed of orbital 1 (green line) and orbital 2 (red line), (b) $\chi^s(\mathbf{q}, 0)$ in the RPA, (c) $\chi_{x^2-y^2}^Q(\mathbf{q}, 0)$ in the SC-VC method (solid red line) and the RPA (black dotted line), and (d) $\chi_{xy}^Q(\mathbf{q}, 0)$ in the SC-VC method (solid green line) and the RPA (black dotted line) for $n = 1.0$.

strong intraorbital nesting between the hole FSs and the electron FSs. For $n = 1.0$, $\chi_{x^2-y^2}^Q$ with peak at $\mathbf{q} = (0, 0)$ is dominant over χ^s and χ_{xy}^Q , which is consistent with the nematic order (fluctuation) in low-doped iron-based superconductors. $\chi_{x^2-y^2}^Q(\mathbf{0}, 0)$ is enhanced by the AL terms $X_{11,11}^{AL,c}(\mathbf{0}, 0)$, $X_{22,22}^{AL,c}(\mathbf{0}, 0)$ in Eq. (6). $X_{11,11(22,22)}^{AL,c}(\mathbf{0}, 0)$ is mainly enlarged by the intraorbital spin fluctuation terms $V_{11,11(22,22)}^s[\mathbf{Q}_1(\mathbf{Q}_2), 0]V_{11,11(22,22)}^s[-\mathbf{Q}_1(-\mathbf{Q}_2), 0]$, where $\mathbf{Q}_1 = (0, \pi)$ and $\mathbf{Q}_2 = (\pi, 0)$ are the nesting vectors for orbitals 1 and 2, respectively. The enhancement of $\chi_{xy}^Q(\mathbf{q}, 0)$ around $\mathbf{Q}_3 = (\pi, \pi)$ is caused by the AL terms $X_{12,12}^{AL,c}(\mathbf{Q}_3, 0)$, $X_{21,21}^{AL,c}(\mathbf{Q}_3, 0)$. $X_{12,12(21,21)}^{AL,c}(\mathbf{Q}_3, 0)$ is mainly enlarged by the terms $V_{11,11(22,22)}^s[\mathbf{Q}_1(\mathbf{Q}_2), 0]V_{12,12(21,21)}^s[\mathbf{Q}_2(\mathbf{Q}_1), 0]$ and $V_{11,11(22,22)}^c(\mathbf{0}, 0)V_{12,12(21,21)}^c(\mathbf{Q}_3, 0)$ in Eq. (6).

Figure 3 shows the results for $n = 1.2$. χ^s has a peak around $\mathbf{q} = (\pi, \pi/5), (\pi/5, \pi)$ due to the intraorbital nesting between the hole FSs and the electron FSs. This incommensurate spin fluctuation originates from the large difference in diameter between the hole FSs and the electron-FSs. In this filling, χ^s is dominant over $\chi_{x^2-y^2}^Q$ and χ_{xy}^Q . The enhancement of $\chi_{x^2-y^2}^Q$

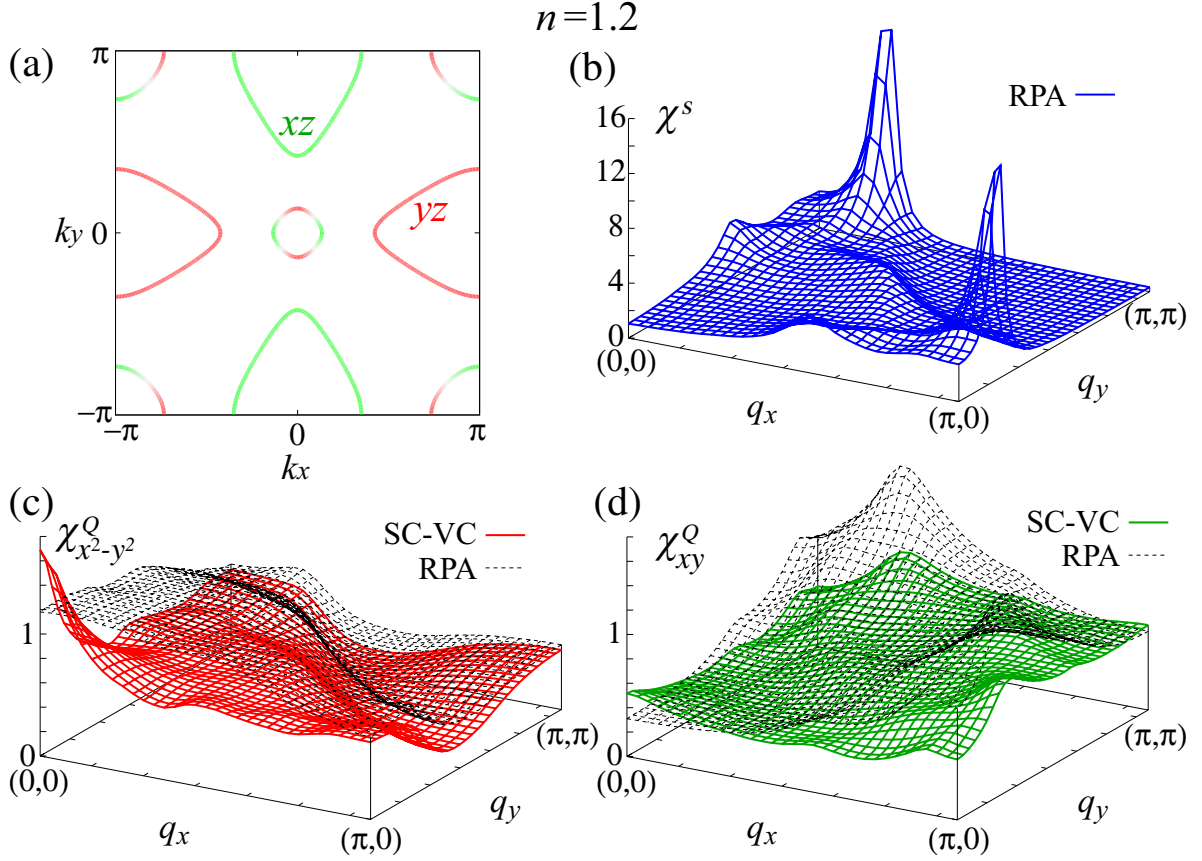


Fig. 3. (Color online) (a) FS composed of orbital 1 (green line) and orbital 2 (red line), (b) $\chi^s(\mathbf{q}, 0)$ in the RPA, (c) $\chi_{x^2-y^2}^O(\mathbf{q}, 0)$ in the SC-VC method (solid red line) and the RPA (black dotted line), and (d) $\chi_{xy}^O(\mathbf{q}, 0)$ in the SC-VC method (solid green line) and the RPA (black dotted line) for $n = 1.2$.

and χ_{xy}^O by the VC is small.

In Fig. 4, we show the results for $n = 0.7$, where the electron FSs disappear. χ^s has a small peak around $\mathbf{Q}_4 = (\pi/2, \pi/2)$ due to the weak nesting between two hole FSs. In this filling, χ_{xy}^O is dominant over χ^s and $\chi_{x^2-y^2}^O$. The enhancement of $\chi_{x^2-y^2}^O$ around $\mathbf{Q}_3 = (\pi, \pi)$ in the SC-VC method is explained by the AL terms $X_{11,11(22,22)}^{AL,c}(\mathbf{Q}_3, 0)$. $X_{11,11(22,22)}^{AL,c}(\mathbf{Q}_3, 0)$ is mainly enlarged by the term $V_{11,11(22,22)}^s(\mathbf{Q}_4, 0)V_{11,11(22,22)}^s(\mathbf{Q}_4, 0)$.

Here, we discuss the reason why the ferro-orbital fluctuation χ_{xy}^O with the peak at $\mathbf{q} = (0, 0)$ is dominant for $n = 0.7$. We introduce the d_{XZ} orbital denoted by the 45°-rotated d_{xz} orbital and the d_{YZ} orbital denoted by the 45°-rotated d_{yz} orbital. Figure 5 shows the FSs composed of the d_{XZ} and d_{YZ} orbitals for $n = 0.7$. We see that the nesting vector $\mathbf{q} \sim (\pi/2, \pi/2)$ is caused by the intraorbital nesting as shown by the blue two-way arrow in Fig. 5. From the analogy of the case for $n = 1.0$, the intraorbital nesting induces the ferro-orbital fluctuation $\chi_{x^2-y^2}^O$ defined in the 45° rotated basis. Thus, the ferro-orbital fluctuation χ_{xy}^O , which is identi-

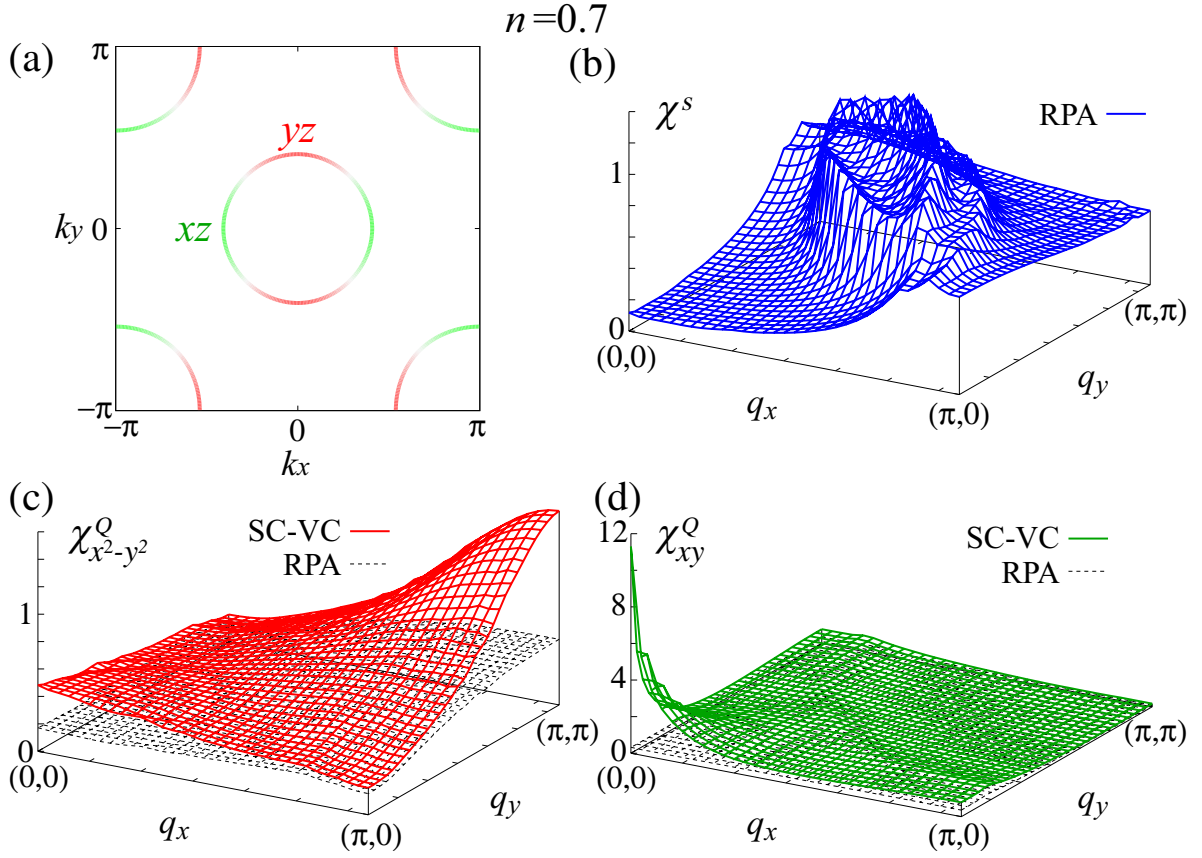


Fig. 4. (Color online) (a) FSs composed of orbital 1 (green line) and orbital 2 (red line), (b) $\chi^s(\mathbf{q}, 0)$ in the RPA, (c) $\chi_{x^2-y^2}^O(\mathbf{q}, 0)$ in the SC-VC method (solid red line) and the RPA (black dotted line), and (d) $\chi_{xy}^O(\mathbf{q}, 0)$ in the SC-VC method (solid green line) and the RPA (black dotted line) for $n = 0.7$.

cal to the ferro-orbital fluctuation $\chi_{x^2-y^2}^O$, is dominant for $n = 0.7$. The orbital dependence of FSs is important for determining the dominant orbital fluctuation.

From these results, we confirmed that dominant fluctuations strongly depend on the topology and the shape of FSs. We also confirmed that dominant fluctuations are valid for the small change in the band parameters. Only the boundary, where dominant fluctuation changes, depends on the band parameters.

4. Summary

We studied the orbital fluctuations near the orbital ordered state using the SC-VC method in the two-orbital (d_{xz} , d_{yz}) Hubbard model. We clarified that the nematic order in the non-doped iron-based superconductors is explained by the two-orbital model around half filling $n = 1.0$. Thus, the d_{xy} orbital is not essential to realize the nematic order. Moreover, the 45° -rotated nematic order appears in the heavily hole-doped case. We confirmed that the

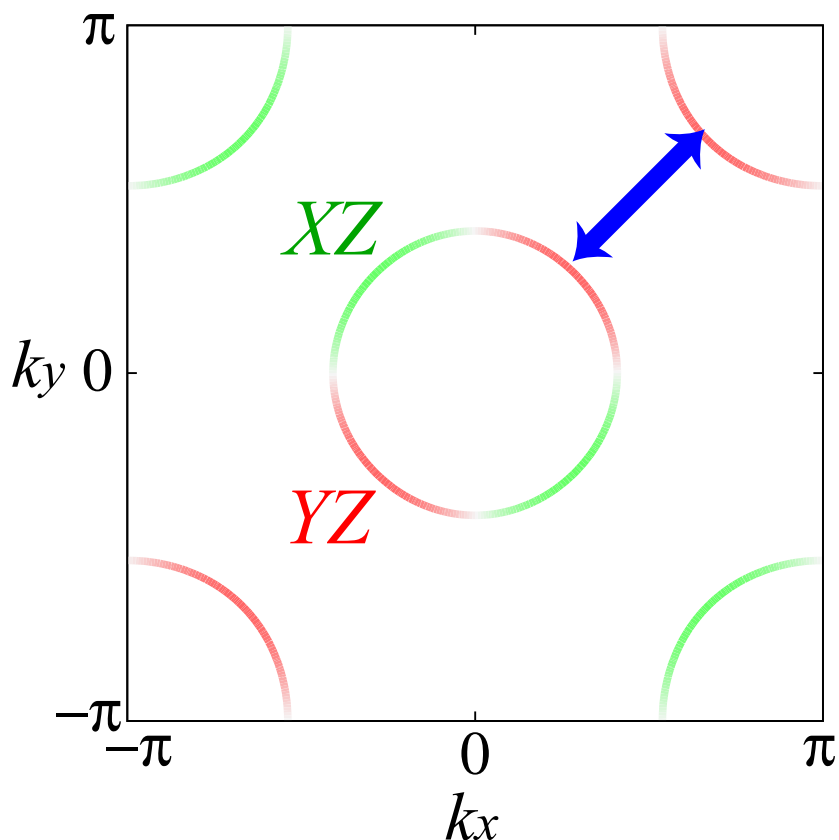


Fig. 5. (Color online) FSs composed of d_{XZ} orbital (green line) and d_{YZ} orbital (red line) for $n = 0.7$. The blue two-way arrow denotes the nesting vector between the two hole FSs.

dominant orbital fluctuation is determined by the orbital dependence and the topology of the Fermi surfaces.

Acknowledgment

We are grateful to H. Kontani for valuable discussions. This work was supported by JSPS KAKENHI Grant Number JP17K05543. Part of numerical calculations was performed on the Yukawa Institute Computer Facility.

References

- 1) S. Nandi, M. G. Kim, A. Kreyssig, R. M. Fernandes, D. K. Pratt, A. Thaler, N. Ni, S. L. Bud'ko, P. C. Canfield, J. Schmalian, R. J. McQueeney, and A. I. Goldman, *Phys. Rev. Lett.* **104**, 057006 (2011).
- 2) H. Luetkens, H.-H. Klauss, M. Kraken, F. J. Litterst, T. Dellmann, R. Klingeler, C. Hess, R. Khasanov, A. Amato, C. Baines, M. Kosmala, O. J. Schumann, M. Braden, J. Hamann-Borrero, N. Leps, A. Kondrat, G. Behr, J. Werner, and B. Büchner, *Nat. Mater.* **8**, 305 (2009).
- 3) R. M. Fernandes, L. H. VanBebber, S. Bhattacharya, P. Chandra, V. Keppens, D. Mandrus, M. A. McGuire, B. C. Sales, A. S. Sefat, and J. Schmalian, *Phys. Rev. Lett.* **105**, 157003 (2010).
- 4) R. M. Fernandes, E. Abrahams, and J. Schmalian, *Phys. Rev. Lett.* **107**, 217002 (2011).
- 5) S. Onari and H. Kontani, *Phys. Rev. Lett.* **109**, 137001 (2012).
- 6) S. Onari, Y. Yamakawa, and H. Kontani, *Phys. Rev. Lett.* **112**, 187001 (2014).
- 7) H. Kontani and S. Onari, *Phys. Rev. Lett.* **104**, 157001 (2010).
- 8) H. Kontani, T. Saito, and S. Onari, *Phys. Rev. B* **84**, 024528 (2011).
- 9) F. Krüger, S. Kumar, J. Zaanen, and J. van den Brink, *Phys. Rev. B* **79**, 054504 (2009).
- 10) W. Lv, J. Wu, and P. Phillips, *Phys. Rev. B* **80**, 224506 (2009).
- 11) C.-C. Lee, W.-G. Yin, and W. Ku, *Phys. Rev. Lett.* **103**, 267001 (2009).
- 12) Y. Yamakawa, S. Onari, and H. Kontani, *Phys. Rev. X* **6**, 021032 (2016).
- 13) Y. Suzuki, T. Shimojima, T. Sonobe, A. Nakamura, M. Sakano, H. Tsuji, J. Omachi, K. Yoshioka, M. Kuwata-Gonokami, T. Watashige, R. Kobayashi, S. Kasahara, T. Shibauchi, Y. Matsuda, Y. Yamakawa, H. Kontani, and K. Ishizaka, *Phys. Rev. B* **92**, 205117 (2015).
- 14) S. Onari, Y. Yamakawa, and H. Kontani, *Phys. Rev. Lett.* **116**, 227001 (2016).
- 15) T. Saito, S. Onari, and H. Kontani, *Phys. Rev. B* **82**, 144510 (2010).
- 16) T. Saito, S. Onari, and H. Kontani, *Phys. Rev. B* **83**, 140512(R) (2011).
- 17) Y. Yamakawa and H. Kontani, *Phys. Rev. Lett.* **114**, 257001 (2015).
- 18) M. Tsuchiizu, Y. Yamakawa, and H. Kontani, *Phys. Rev. B* **93**, 155148 (2016).
- 19) M. Tsuchiizu, Y. Ohno, S. Onari, and H. Kontani, *Phys. Rev. Lett.* **111**, 057003 (2013).

- 20) Y. Ohno, M. Tsuchiizu, S. Onari, and H. Kontani, J. Phys. Soc. Jpn. **82**, 013707 (2013).
- 21) M. Tsuchiizu, Y. Yamakawa, S. Onari, Y. Ohno, and H. Kontani, Phys. Rev. B **91**, 155103 (2015).
- 22) S. Raghu, X.-L. Qi, C.-X. Liu, D. J. Scalapino, and S.-C. Zhang, Phys. Rev. B **77**, 220503(R) (2008).
- 23) S. Onari and H. Kontani, in *Iron-Based Superconductivity*, ed. P.D. Johnson, G. Xu, and W.-G. Yin, (Springer Verlag Berlin and Heidelberg GmbH & Co. K, 2015) p. 331.
- 24) T. Miyake, K. Nakamura, R. Arita, and M. Imada, J. Phys. Soc. Jpn. **79**, 044705 (2010).